

Forward-Backward Asymmetries of Fourth Family Fermions Through the Z' Models at Linear Colliders

V. Ari,^{*} O. Çakir,[†] and V. Çetinkaya[‡]

Ankara University, Faculty of Sciences,

Department of Physics, 06100, Tandogan, Ankara.

Abstract

We investigate the forward-backward asymmetries in the pair production of fourth family fermions through the new Z' interactions in the e^+e^- collisions. The Z' boson having family universal couplings can contribute to the pair production of fourth family fermions via the s -channel exchange. The linear colliders will provide a clean environment for the physics of Z' boson to measure its couplings precisely. The effects of the Z' boson to the asymmetries are shown to be important in some parameter regions for different Z' models. Among these parameters, the invariant mass distribution $m_{F\bar{F}}$ will be an important measurement to constrain the Z' models. Providing the fourth family fermion exist in an accessible mass range, a χ^2 analysis can also be used to probe the Z' models at linear collider energies.

^{*}Electronic address: volkan.ari@science.ankara.edu.tr

[†]Electronic address: ocakir@science.ankara.edu.tr

[‡]Electronic address: volkan.cetinkaya@science.ankara.edu.tr

I. INTRODUCTION

Even though we observe three families of quarks and leptons of the Standard Model (SM), however there could be a fourth family if their masses are beyond our present experimental reach. A family extension to the SM fermion families contains the quarks t' and b' , and charged lepton l' with its associated neutrino ν' . The allowed parameter space for a fourth family is restricted by the experimental searches, precision electroweak measurements, theoretical constraints from the requirements of unitarity and perturbativity. Data from the experiments at Tevatron restricts the masses of t' and b' quarks in the fourth family: $M_{t'} > 335$ GeV at 95% CL. [1] assuming $t' \rightarrow W^+q$ (where $q = d, s, b$) and $M_{b'} > 338$ GeV at 95% CL. [2] assuming $b' \rightarrow W^-t$. However, in some mixing scenarios the lower limit on the t' mass increases to $M_{t'} \gtrsim 400$ GeV [3]. From direct production searches at LEP II, there is a lower limit of the order of 100 GeV for the fourth family charged lepton and unstable neutrino. The precision measurements restrict the mass splitting between the fourth family leptons $|M_{l'} - M_{\nu'}| \approx 30 - 60$ GeV and the fourth family quarks $|M_{t'} - M_{b'}| \approx 50 - 70$ GeV [4, 5].

The fourth family quarks and leptons could also couple to an extra neutral gauge boson different from the three SM families. A new neutral gauge boson Z' can have family universal or non-universal couplings to fermions. The indirect searches of the Z' boson can also be performed at linear colliders where the discovery limits are related to the deviations from the SM predictions for the cross sections and asymmetries due to the interference effects between the propagators. The Z' boson having family universal couplings can contribute to the pair production of fourth family fermions via the s -channel exchange. The linear collider provides a clean environment for Z' physics, and can measure the couplings precisely.

In the extensions of the SM with $U(1)_\psi \times U(1)_\chi$ gauge symmetry, the fields Z'_ψ and Z'_χ can be massive and their states can mix, therefore, a relatively lighter mass eigenstate can be written as $Z'(\theta) = Z'_\psi \cos \theta + Z'_\chi \sin \theta$. A set of Z' models have some special names: the sequential Z'_S model has the same coupling to the fermions as that of the Z boson of the SM; the Z'_ψ , Z'_χ and Z'_η models corresponding to the specific values of the mixing angle θ (0, $\pi/2$ and $\arctan \sqrt{3/5}$, respectively) in the E_6 model have different couplings to the fermions; the Z'_{B-L} model has the couplings related to the minimal $B - L$ (where B and L are baryon and lepton numbers, respectively) extension of the SM. The detailed descriptions

of the Z' models, as well as the specific references can be found in Refs. [6–9]. The current experimental searches of the Z' boson from Drell-Yan cross sections at Tevatron have put lower limits on the mass range $0.6 - 1.0$ TeV at 95% C.L. depending on the specific Z' models [10]. From the electroweak precision data analysis, the improved lower limits on the Z' mass are given in the range $1.1 - 1.4$ TeV at 95% C.L. [11]. These limits on the Z' boson mass favors higher energy (≥ 1 TeV) collisions for direct observation of the signal. It is also possible that the Z' bosons can be much heavy or weak enough to escape beyond the discovery reach expected at the LHC. In this case, only the indirect signatures of Z' exchanges may occur at the high energy colliders.

Recently, D0 and CDF Collaborations have measured the forward-backward (FB) asymmetries of top quark A_{FB}^t at Tevatron [12, 13] in the large $t\bar{t}$ invariant mass region, while the A_{FB}^b was measured in the Z boson decays at LEP [14], which differ by about 3σ deviations from the SM expectations, without affecting significantly the well behaved total cross sections. Several models of new physics have been considered to explain these asymmetries (see Refs. [15–17] and references therein) at hadron colliders.

In this study, we investigate the forward-backward asymmetries A_{FB}^F for pair production of the fourth family fermions F_i (t', b', l', ν') within the Z' models at linear collider energies of 1 TeV and 3 TeV. The linear colliders, namely the International Linear Collider (ILC) described in [19] and the Compact Linear Collider (CLIC) described in [21], have been designed to meet the basic parameters required for the planned physics programs [20] and [22], respectively. The effects of the Z' boson to the asymmetries of fourth family fermions at linear colliders are shown to be important in some parameter regions for the sequential model, some special E6 models and the $B - L$ model. We will typically consider the mass of the fourth family charged lepton greater than 200 GeV and the masses of the fourth family quarks greater than 350 GeV, which are safely above the direct production bounds.

II. INTERACTIONS WITH FOURTH FAMILY FERMIONS

The interactions of the fourth family quarks (Q_i) via neutral gauge bosons (g, γ, Z, Z') and fourth family leptons (L_i) via electroweak gauge bosons (γ, Z, Z') can be described by the following Lagrangian. We also include the interactions of fourth family fermions (F_i) with three known families of fermions (f_i) through the charged currents (via W^\pm bosons)

Table I: The family independent vector and axial-vector couplings to new Z' boson predicted by different models.

down-type quarks		up-type quarks		charged leptons		neutrinos	
C'_V	C'_A	C'_V	C'_A	C'_V	C'_A	C'_V	C'_A
Z'_S							
$-\frac{1}{2} + \frac{2}{3} \sin^2 \theta_W$	$-\frac{1}{2}$	$\frac{1}{2} - \frac{4}{3} \sin^2 \theta_W$	$\frac{1}{2}$	$-\frac{1}{2} + 2 \sin^2 \theta_W$	$-\frac{1}{2}$	$\frac{1}{2}$	$\frac{1}{2}$
Z'_ψ							
0	$\frac{\sqrt{10}}{6} \sin \theta_W$	0	$\frac{\sqrt{10}}{6} \sin \theta_W$	0	$\frac{\sqrt{10}}{6} \sin \theta_W$	$\frac{\sqrt{10}}{12} \sin \theta_W$	$\frac{\sqrt{10}}{12} \sin \theta_W$
Z'_χ							
$\frac{\sqrt{6}}{3} \sin \theta_W$	$-\frac{\sqrt{6}}{6} \sin \theta_W$	0	$\frac{\sqrt{6}}{6} \sin \theta_W$	$-\frac{\sqrt{6}}{3} \sin \theta_W$	$-\frac{\sqrt{6}}{6} \sin \theta_W$	$-\sqrt{6} \sin \theta_W$	$-\sqrt{6} \sin \theta_W$
Z'_η							
$\sin \theta_W$	$\frac{1}{3} \sin \theta_W$	0	$4 \sin \theta_W$	$-\sin \theta_W$	$\frac{1}{3} \sin \theta_W$	$-\frac{1}{3} \sin \theta_W$	$-\frac{1}{3} \sin \theta_W$
Z'_{B-L}							
$\frac{2}{3}$	0	$\frac{2}{3}$	0	-2	0	-1	-1

to be read as

$$\begin{aligned}
L' = & -g_s \bar{Q}_i T^a \gamma^\mu Q_i G_\mu^a - g_e Q_F \bar{F}_i \gamma^\mu F_i A_\mu - \frac{g}{2\sqrt{2}} V_{ij} \bar{F}_i \gamma^\mu (1 - \gamma^5) f_j W_\mu \\
& - \frac{g_Z}{2} \bar{F}_i \gamma^\mu (C_V^F - C_A^F \gamma^5) F_i Z_\mu - \frac{g_{Z'}}{2} \bar{F}_i \gamma^\mu (C_V^{F'} - C_A^{F'} \gamma^5) F_i Z'_\mu + \text{H.c.}
\end{aligned} \quad (1)$$

where g_s , g_e , g_Z are the strong, electromagnetic and weak-neutral coupling constants, respectively. The G_μ^a , A_μ , W_μ and Z_μ are the fields for gluons, photon, W and Z bosons, respectively. The C'_V (C_V) and C'_A (C_A) are vector and axial-vector couplings with the Z' (Z) boson and they are given in Table I.

The decay widths into the heavy fermion pair $F\bar{F}$ and W^+W^- bosons are given as

$$\Gamma(Z' \rightarrow F\bar{F}) = \frac{g_{Z'}^2 N_c}{48\pi M_{Z'}} \sqrt{1 - \frac{4M_F^2}{M_{Z'}^2}} \left[(C_A^{F'})^2 (-4M_F^2 + M_{Z'}^2) + (C_V^{F'})^2 (M_{Z'}^2 + 2M_F^2) \right] \quad (2)$$

$$\begin{aligned}
\Gamma(Z' \rightarrow W^+W^-) = & \frac{g_W^2 \cos^2 \theta_W \kappa^2}{192\pi M_{Z'} M_W^4} \sqrt{1 - \frac{4M_W^2}{M_{Z'}^2}} \left(\frac{M_Z}{M_{Z'}} \right)^4 \\
& \times [M_{Z'}^6 + 16M_W^2 M_{Z'}^4 - 68M_W^4 M_{Z'}^2 - 48M_W^6]
\end{aligned} \quad (3)$$

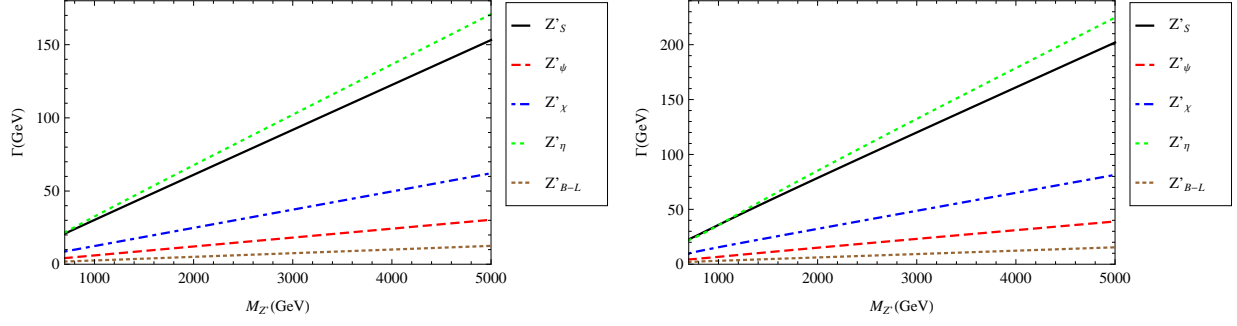


Figure 1: The decay widths of Z' boson predicted by different models in the case of three (left) and four (right) fermion families.

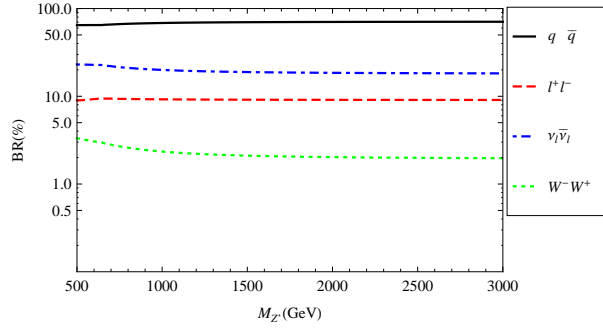


Figure 2: The branching ratios of Z' boson predicted by different models depending on its mass.

where N_c is the color factor (3 for quarks and 1 for leptons), and $g_{Z'}$ is the coupling constant for Z' boson. The M_Z , $M_{Z'}$ and M_W are the masses for Z , Z' and W bosons, respectively. The M_F is the mass of heavy fermion. The mixing term between the Z' boson and Z boson is assumed to be of the order of $M_Z^2/M_{Z'}^2$, hence a mixing factor κ scales this extension depending on the specific Z' models. In the sequential model the factor κ is chosen to be unity, which is a reference for the purpose of comparison. In Fig. 1 we present the decay width of Z' boson versus the mass $M_{Z'}$ in case of three and four fermion families. As it can be seen from Fig. 1 that the total decay width of the sequential Z' boson is about 90 GeV for three families and 120 GeV for four families at a mass value of $M_{Z'} = 3000$ GeV. It turns out that the branching ratios of all fermionic modes are not sensitive to $M_{Z'}$, leading to the fractions of about 0.7, 0.2, 0.1 and 0.02 for $Z' \rightarrow q\bar{q}$, $Z' \rightarrow \nu\bar{\nu}$, $Z' \rightarrow l^+l^-$ and $Z' \rightarrow W^+W^-$, respectively for the sequential Z' model. Here, the $q\bar{q}$ mode includes the quarks of four families, and the $l^+l^- (\nu\bar{\nu})$ mode includes the charged leptons(neutrinos) of four families.

Table II: The cross sections (fb) for the fourth family pair production processes (without Z') at CLIC with $\sqrt{s} = 3$ TeV. The numbers in paranthesis shows the results for ILC with $\sqrt{s} = 1$ TeV.

Mass (GeV)	$e^+e^- \rightarrow \nu'\bar{\nu}'$	$e^+e^- \rightarrow l'^+l'^-$	Mass (GeV)	$e^+e^- \rightarrow b'\bar{b}'$	$e^+e^- \rightarrow t'\bar{t}'$
100	2.74(24.36)	12.47(111.70)	300	9.93(71.00)	19.70(153.00)
200	2.71(22.10)	12.44(108.60)	400	9.74(51.50)	19.40(121.00)
300	2.67(18.28)	12.39(100.70)	500	9.48	19.20
400	2.60(12.66)	12.31(81.80)	600	9.17	18.80
500	2.52	12.20	700	8.79	18.30
600	2.42	12.05	800	8.35	17.70
700	2.29	11.84	900	7.83	17.00
800	2.16	11.56	1000	7.22	16.10

III. CROSS SECTIONS

Using the interaction Lagrangian (1) we calculate the differential cross section for the pair production of fourth family quarks and leptons in the collisions of e^+ and e^- beams. The analytical expressions for the differential cross section are given in the Appendix. We calculate the cross section for pair production of fourth family quarks (leptons) taking their masses in the interval 300-1000 (200-800) GeV. Table II shows the production cross sections without Z' contribution at ILC and CLIC energies. The ILC with $\sqrt{s} = 1$ TeV has advantageous up to the kinematical range ($m_F \leq 500$ GeV) for the pair production cross section. However, the CLIC with $\sqrt{s} = 3$ TeV extends the mass range for the fourth family fermions. In order to see the contributions from Z' boson exchange and its interference we also calculate the cross sections assuming the reference mass values $M_{b'} = 350$ GeV and $M_{\nu'} = 100$ GeV with the constraints $M_{t'} \approx M_{b'} + 50$ GeV and $M_{l'} \approx M_{\nu'} + 100$ GeV. These cross sections are shown in Table III for ILC with $\sqrt{s} = 1$ TeV and in Table IV for CLIC with $\sqrt{s} = 3$ TeV within different Z' models. Here, we assume the Z' boson mass $m_{Z'} = 1500$ TeV.

The leptonic decay mode of the Z' boson has lower branching ratio than the hadronic one, but the cross section for the process $e^-e^+ \rightarrow l'^-l'^+$ is comparable with the $t'\bar{t}'$ pair production for some Z' models. The intermediate goals after the discovery of the Z' boson and the fourth family fermions would be to understand their properties and couplings. The forward-backward asymmetry and the invariant mass spectrum of the heavy fermions could

Table III: The cross sections for the processes $e^-e^+ \rightarrow F\bar{F}$ (where $F = t', b', l', \nu'$) at the collision center of mass energy $\sqrt{s} = 1$ TeV.

Cross sections(fb)	Z'_S	Z'_ψ	Z'_χ	Z'_η	Z'_{B-L}
$e^-e^+ \rightarrow t'\bar{t}'$	106.29	124.35	119.05	128.60	112.20
$e^-e^+ \rightarrow b'\bar{b}'$	31.55	57.44	113.19	72.57	67.70
$e^-e^+ \rightarrow l'^-\bar{l}'^+$	98.98	105.04	75.64	96.11	93.14
$e^-e^+ \rightarrow \nu'\bar{\nu}'$	1.15	29.55	38.65	23.70	22.76

Table IV: The same as Table III, but for $\sqrt{s} = 3$ TeV.

Cross section (fb)	Z'_S	Z'_ψ	Z'_χ	Z'_η	Z'_{B-L}
$e^-e^+ \rightarrow t'\bar{t}'$	39.10	17.40	22.00	23.31	21.54
$e^-e^+ \rightarrow b'\bar{b}'$	35.94	12.87	6.81	8.58	8.85
$e^-e^+ \rightarrow l'^-\bar{l}'^+$	18.47	13.51	20.99	15.05	15.65
$e^-e^+ \rightarrow \nu'\bar{\nu}'$	14.90	1.89	2.11	2.92	2.76

help to identify the nature of these new particles.

IV. FORWARD-BACKWARD ASYMMETRY

The forward-backward asymmetry A_{FB} is defined as the relative difference between the cross sections with $\cos \theta > 0$ and $\cos \theta < 0$, being θ the angle between the heavy fermion F and initial electron in the center of mass frame:

$$A_{FB} = \frac{\sigma(\cos \theta > 0) - \sigma(\cos \theta < 0)}{\sigma(\cos \theta > 0) + \sigma(\cos \theta < 0)}$$

Since the photon has only vector-like couplings to charged fermions the photon exchange can not generate an asymmetry, while the Z boson and Z' boson exchange and their interference can generate asymmetry for the fourth family fermions. If the heavy fermions are localized differently along a new dynamical symmetry breaking, one can then expect that the interactions of heavy fermions can be different from the ones of the light fermions. The presence of the s -channel resonance in $F\bar{F}$ production could be identified by an examination of the invariant mass distributions with sufficient statistics. It is seen from Figs. 3 and 4

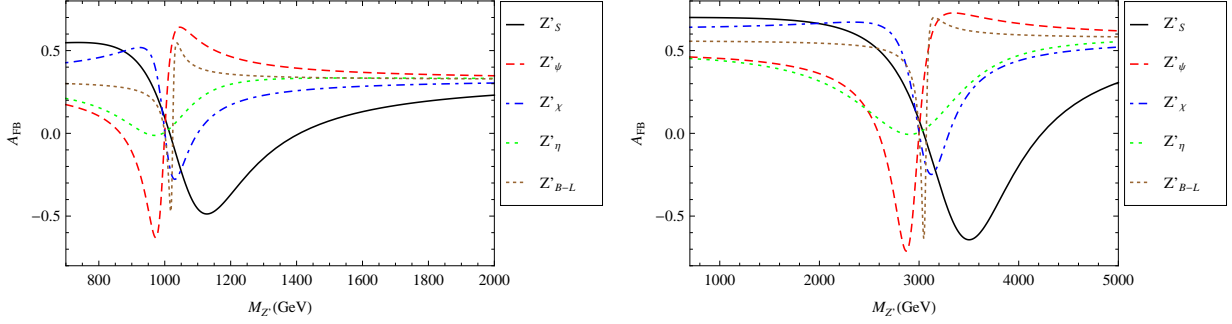


Figure 3: Forward-backward asymmetry for t' quark within different Z' models at the center of mass energies 1 TeV (left) and 3 TeV (right).

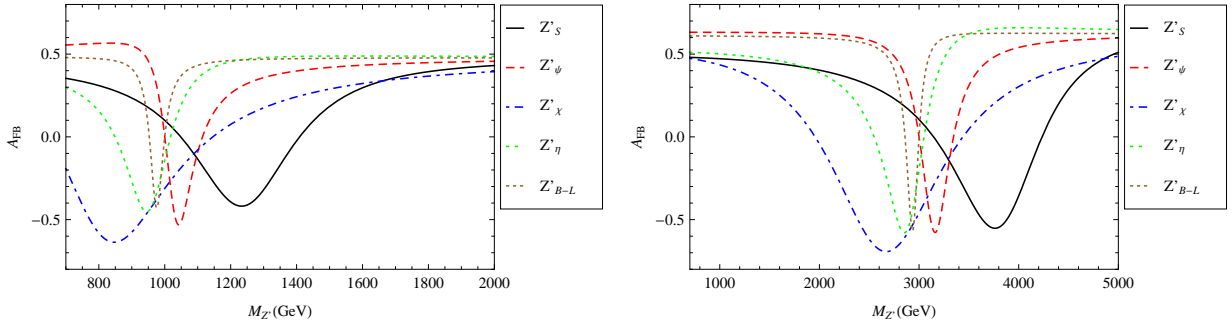


Figure 4: The same as Fig. 3, but for b' quark.

that the asymmetry changes sign at a value of the $M_{Z'}$ near the center of mass energy. Figs. 5 and 6 show the asymmetries for the fourth family leptons depending on the Z' mass. At relatively low $M_{Z'}$ the asymmetry value is around 0.55 (0.7) for t' pair production with the contribution of sequential Z' boson at the center of mass energy of 1 (3) TeV. While it has the value around 0.25 (0.3) for the large mass region at $\sqrt{s}=1$ (3) TeV.

In order to see how the asymmetry changes depending on the heavy fermion mass M_F we plot Fig. 7 without Z' contribution. For the forward-backward asymmetry of the fourth family fermions depending on the invariant mass ($M_{F\bar{F}}$) cut and the initial state radiation (ISR) and beamstrahlung (BS) effects, we use CalcHEP [23] with the beam parameters for the ILC [19] and CLIC [21] as presented in Table V.

The asymmetries (A'_{FB}) defined in terms of differential cross sections are presented in Fig. 8 depending on the invariant mass of heavy fermions for $M_{Z'} = 3500$ GeV at CLIC with $\sqrt{s} = 3$ TeV. One may compare the distributions between the sequential Z' model

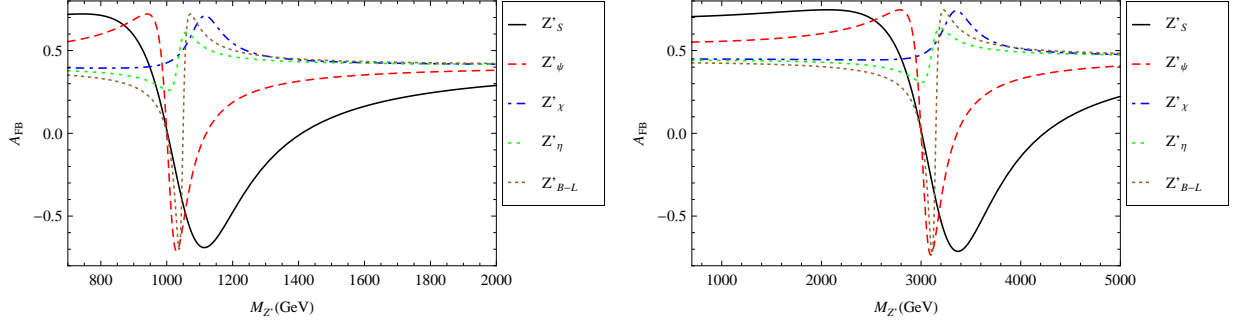


Figure 5: Forward-backward asymmetry for l' lepton within different Z' models at the center of mass energies 1 TeV (left) and 3 TeV (right).

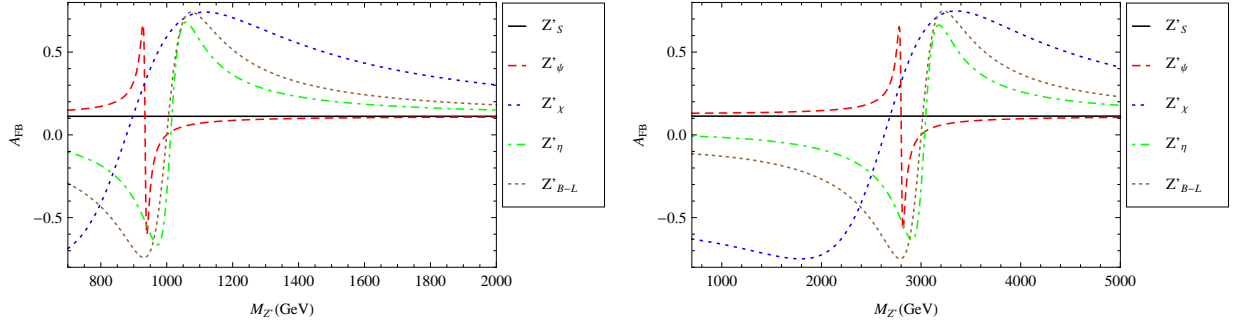


Figure 6: The same as Fig. 5, but for ν' .

and Z'_ψ model. It is seen that Z'_ψ model generates more asymmetry for charged fermions depending on the invariant mass $M_{F\bar{F}}$. One should note that there is a minimum value for the invariant mass distributions of each type of fermions. The value of the minimum will change depending on the value of the heavy fermion mass. The asymmetry for the neutrino

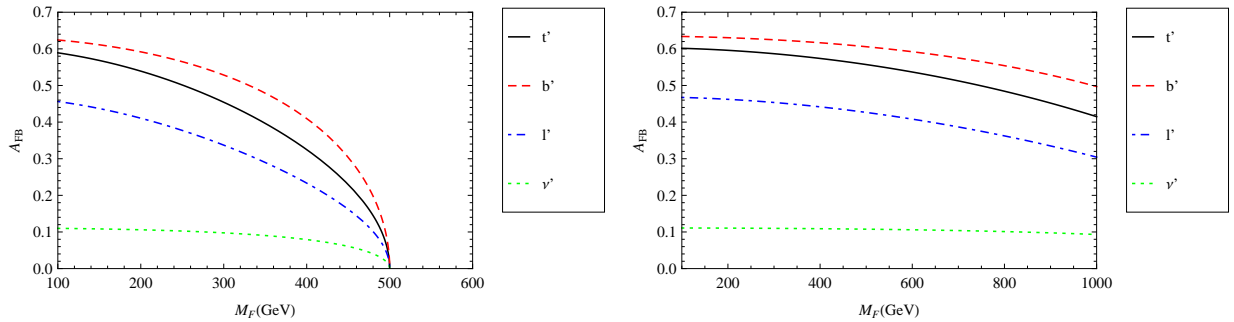


Figure 7: The forward-backward asymmetries for the fourth family quarks (t' , b') and leptons (l' , ν') depending on the heavy fermion mass at $\sqrt{s} = 1$ TeV (left) and $\sqrt{s} = 3$ TeV (right).

Table V: The collider beam parameters of the ILC and CLIC needed to calculate the ISR and BS.

	ILC	CLIC
Horizontal beam size (nm)	640	45
Vertical beam size (nm)	5.7	1
Bunch length (mm)	0.3	0.044
Number of particles in the bunch (N)	2×10^{10}	3.72×10^9
Design luminosity ($\text{cm}^{-2}\text{s}^{-1}$)	2×10^{34}	5.9×10^{34}

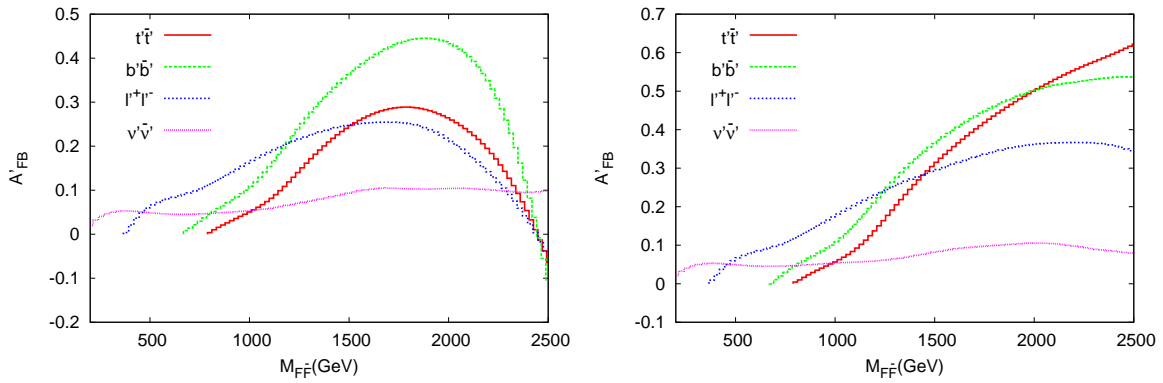


Figure 8: Asymmetry depending on the heavy fermion invariant mass for sequential Z'_S model (left) and Z'_ψ model (right) for $m_{Z'} = 3500$ GeV at CLIC with $\sqrt{s} = 3$ TeV.

remains at the same low level for these models.

V. ANALYSIS

In order to analyze the Z' models we define a χ^2 function given by

$$\chi^2 = \frac{(\sigma^{\text{with } Z'} - \sigma^{\text{no } Z'})^2}{\sigma^{\text{no } Z'} / (BR \epsilon L_{int})}$$

where $\sigma^{\text{with } Z'}$ and $\sigma^{\text{no } Z'}$ are the cross sections for pair production of the fourth family fermions with a Z' boson and without Z' boson, respectively. The integrated luminosity L_{int} is taken as 200 fb^{-1} at the center of mass energy $\sqrt{s} = 1$ TeV and 600 fb^{-1} at $\sqrt{s} = 3$ TeV. The BR and ϵ correspond to the branching ratio and efficiency for considered decay mode, respectively.

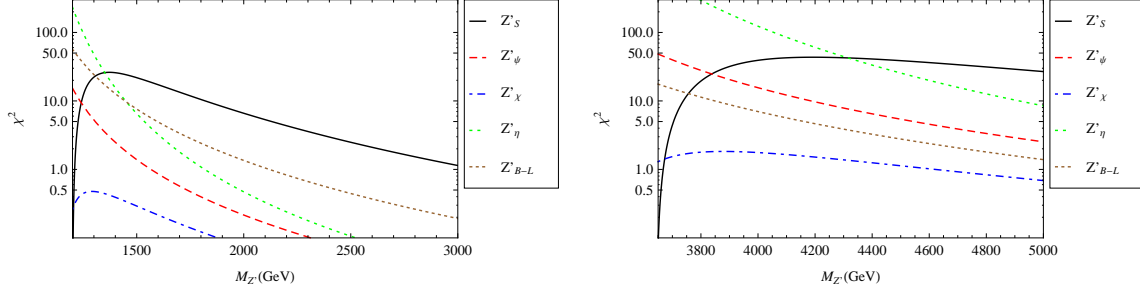


Figure 9: The χ^2 distribution for t' pair production process depending on the Z' mass at $\sqrt{s} = 1$ TeV (left) and $\sqrt{s} = 3$ TeV (right).

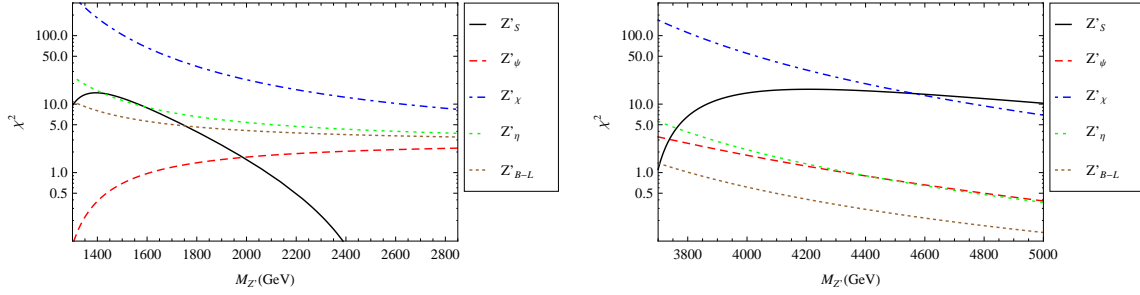


Figure 10: The same as Fig. 9, but for the b' pair production at $\sqrt{s} = 1$ TeV (left) and $\sqrt{s} = 3$ TeV (right).

First, we take into account the pair production of fourth family quarks (t' and b') and their decays via $t'\bar{t}' \rightarrow W^+bW^-\bar{b}$ and $b'\bar{b}' \rightarrow W^-tW^+\bar{t} \rightarrow W^-W^+bW^+W^-\bar{b}$, respectively. For t' pair production process, we consider the leptonic decay of one W boson and hadronic decay of the other W boson giving the signal $l^\pm + 2b_{jet} + 2j + \text{MET}$. In Fig. 9, we plot the χ^2 distribution versus $M_{Z'}$ assuming the mass value $m_{t'} = 400$ GeV and CKM4 elements $V_{t'b'} = 0.993$, $V_{t'b} = 0.108$, $V_{t's} = 0.031$, $V_{t'd} = 0.009$, $V_{tb'} = 0.107$, $V_{cb'} = 0.030$, $V_{ub'} = 0.016$ [24] at the linear collider center of mass energies $\sqrt{s} = 1$ TeV and 3 TeV. For b' pair production, we take into account the same sign W bosons decay leptonically, while the others decay hadronically, leading to the signal $2l^\pm + 2b_{jet} + 4j + \text{MET}$. In Fig. 10, the χ^2 distribution versus $M_{Z'}$ assuming the mass value $m_{b'} = m_{t'} - 50$ GeV at the linear collider center of mass energies $\sqrt{s} = 1$ TeV and 3 TeV.

For $t'(b')$ pair production we can identify the Z'_S model in the mass range of $1250 < m_{Z'} < 2200$ GeV ($1250 < m_{Z'} < 1800$ GeV) at linear collider energy of $\sqrt{s} = 1$ TeV. A higher center of mass energy $\sqrt{s} = 3$ TeV expands this range to $m_{Z'} > 3700$ GeV. However,

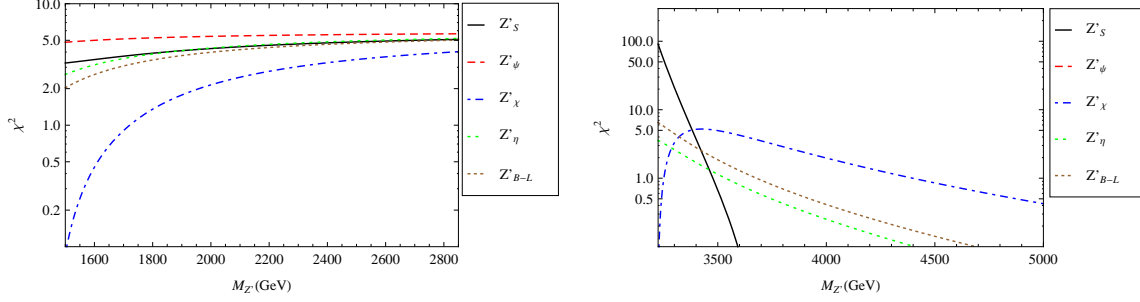


Figure 11: The χ^2 distribution for l' pair production process depending on the Z' mass at $\sqrt{s} = 1$ TeV (left) and $\sqrt{s} = 3$ TeV (right).

the other models can be identified in the smaller mass range. Specifically, for the b' pair production the Z'_χ model will give its signature more pronounced up to 4500 GeV.

Second, we consider the pair production of fourth family charged lepton and neutrino (l' and ν') and their decays via $l'\bar{l}' \rightarrow W^- \nu' W^+ \bar{\nu}' \rightarrow W^- \mu^\mp W^\pm W^+ \mu^\mp W^\pm$ and $\nu'\bar{\nu}' \rightarrow W^\pm \mu^\mp W^\pm \mu^\mp$ assuming the Majorana nature of the neutrino, respectively. For l' pair production, we assume three same sign W bosons decay leptonically, while the other decays hadronically, giving the signal $3l^\pm + 2\mu^\mp + 2j + \text{MET}$. In Fig. 11, we plot the χ^2 distribution versus $M_{Z'}$ assuming the mass value $m_{l'} = 200$ GeV and PMNS4 elements $U_{\nu'l'} > 0.996$ and $U_{\nu'l} < 0.092$ [25] at the collider energies $\sqrt{s} = 1$ TeV and 3 TeV. For ν' pair production, here we assume the W bosons decay hadronically, leading to the signal $2\mu^\pm + 4j$. In Fig. 12, the χ^2 distribution versus $M_{Z'}$ assuming the mass value $m_{\nu'} = m_{l'} - 100$ GeV at the center of mass energies $\sqrt{s} = 1$ TeV and 3 TeV.

In the l' pair production search we can also identify the Z'_ψ model in the mass range $1500 < m_{Z'} < 2800$ GeV, while the other models Z'_S , Z'_η and Z'_{B-L} can be identified in the range of $m_{Z'} \gtrsim 1800$ GeV at $\sqrt{s} = 1$ TeV. For the ν' pair production search most of the models can be identified in the mass range $1300 < m_{Z'} < 2200$ GeV at $\sqrt{s} = 1$ TeV. A higher center of mass energy $\sqrt{s} = 3$ TeV expands this range to $m_{Z'} > 3700$ GeV.

The number of signal events for the fourth family pair production processes at the center of mass energies $\sqrt{s} = 1$ TeV and 3 TeV are given in Table VI and VII, respectively. Here, we take the masses of fourth family quarks as $m_{t'} = m_{b'} + 50$ GeV = 400 GeV and fourth family lepton masses as $m_{l'} = m_{\nu'} + 100$ GeV = 200 GeV. We assume the CKM4 elements given in [24] and PMNS4 elements given in [25]. The corresponding background events are

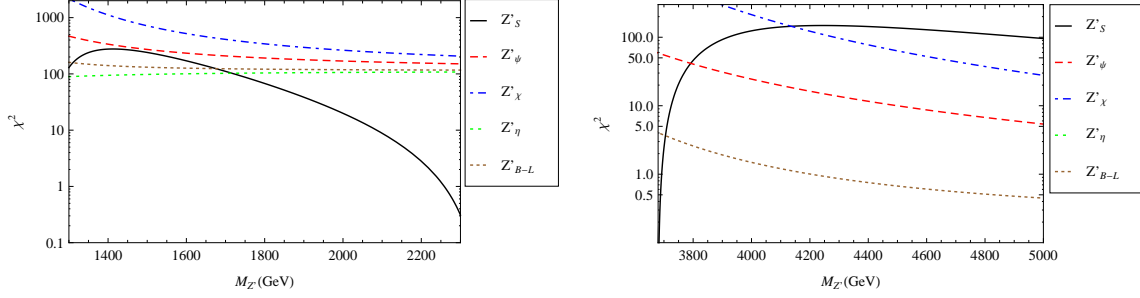


Figure 12: The same as Fig. 11, but for the ν' pair production at $\sqrt{s} = 1$ TeV (left) and $\sqrt{s} = 3$ TeV (right).

Signal	Z'_S	Z'_ψ	Z'_χ	Z'_η	Z'_{B-L}	Background
$t'\bar{t}' \rightarrow l^+ + 2b_j + 2j + \text{MET}$	672.9(20.02)	787.3(175.95)	753.7(56.82)	814.2(108.01)	710.4(68.35)	$W^+bW^-\bar{b}$ 1129.5
$b'\bar{b}' \rightarrow 2l^+ + 2b_j + 4j + \text{MET}$	23.2(59.90)	42.2(5.45)	83.1(35.59)	53.3(8.93)	49.7(16.63)	$W^-tW^+\bar{t}$ 0.15
$l'\bar{l}' \rightarrow 2\mu^- + 3\mu^+ + 2j + \text{MET}$	14.7(103.94)	15.6(1.53)	11.2(9.05)	14.2(74.58)	13.8(24.97)	ZZW^+W^- 0.02
$\nu'\bar{\nu}' \rightarrow 2\mu^- + 4j$	10.9(11.43)	279.9(82.80)	366.0(40.22)	224.4(35.38)	215.6(36.25)	$W^+W^-W^+W^-$ 0.91

Table VI: Number of signal and background events for relevant final states at $\sqrt{s} = 1$ TeV and $L_{int} = 200 \text{ fb}^{-1}$. The numbers in the paranthesis denote corresponding signal significances.

also given in the last column of Table VI and VII for 200 fb^{-1} and 600 fb^{-1} , respectively. When calculating the number of signal and background events we take into account the corresponding branching ratios and the efficiency factors for the given channel of signal. In the final state including b -quarks we take the b -tagging efficiency as $\epsilon = 0.5$.

In order to estimate signal significance for the production of fourth family fermions we use signal and background events at linear colliders with $\sqrt{s} = 1$ TeV and 3 TeV. From the Table VI (VII), for an illustration, we have the signal significances (S/\sqrt{B}) in the framework of Z'_S model as 20.0(28.7), 59.9(73.2), 103.9(23.4) and 11.4(187.5) for the t' , b' , l' and ν' pair

Signal	Z'_S	Z'_ψ	Z'_χ	Z'_η	Z'_{B-L}	Background
$t'\bar{t}' \rightarrow l^+ + 2b_j + 2j + \text{MET}$	730.2(28.67)	324.2(12.73)	409.9(16.09)	435.2(17.09)	402.3(15.80)	$W^+bW^-\bar{b}$ 648.5
$b'\bar{b}' \rightarrow 2l^+ + 2b_j + 4j + \text{MET}$	77.8(73.19)	27.9(26.25)	14.8(13.92)	18.6(17.50)	19.2(18.06)	$W^-tW^+\bar{t}$ 1.13
$l'\bar{l}' \rightarrow 2\mu^- + 3\mu^+ + 2j + \text{MET}$	8.1(23.38)	5.9(17.03)	9.2(26.56)	6.6(19.05)	6.8(19.63)	ZZW^+W^- 0.12
$\nu'\bar{\nu}' \rightarrow 2\mu^- + 4j$	416.3(187.49)	52.7(23.73)	58.8(26.48)	81.5(36.71)	76.4(34.41)	$W^+W^-W^+W^-$ 4.93

Table VII: The same as Table VI, but for $\sqrt{s} = 3$ TeV and $L_{int} = 600 \text{ fb}^{-1}$.

production, respectively. Providing the fourth family fermions exist within the considered mass range, the Z' models can be probed with a large significance at linear colliders.

VI. CONCLUSIONS

We emphasize that exploring the $F\bar{F}$ production cross sections and forward-backward asymmetry at linear colliders will allow further tests of the new models beyond the SM. Taking the masses of fourth family fermions as $m_{t'} = 400$ GeV and $m_{b'} = 200$ GeV with the constraints $m_{t'} - m_{b'} = 50$ GeV and $m_{l'} - m_{\nu'} = 100$ GeV, the CLIC (ILC) can produce fourth family fermions t' , b' , l' and ν' signal events 368(766), 21(38), 5(16), 78(231) per year, respectively. We study the dependence of A_{FB}^F on the heavy fermion invariant mass $M_{F\bar{F}}$. At CLIC (ILC), the forward backward asymmetry for t' , b' , l' and ν' without Z' contribution can be calculated as 0.57(0.32), 0.62(0.48), 0.46(0.41) and 0.11(0.11), respectively. The forward backward asymmetries of fourth family fermions can be affected with the Z' masses in the framework of models. For an invariant mass of $M_{F\bar{F}} \approx 2$ TeV, the t' and b' quarks can produce a forward backward asymmetry of $A'_{FB} = 0.5$ if the Z'_ψ model is realized. However, heavy charged lepton FB asymmetry can also be measured at relatively low invariant mass range. Performing a χ^2 analysis using the cross sections we have the mass range for the Z' boson which can be accessible at the linear collider experiments. We found that the Z' models give different predictions for the observables and their correlations, and they may be distinguished by jointly studying these observables at linear colliders.

APPENDIX

The differential cross section for the process $e^+e^- \rightarrow F\bar{F}$ is given by

$$\begin{aligned} \frac{d\sigma(e^-e^+ \rightarrow F\bar{F})}{dt} = & \frac{1}{16\pi s^2} \left\{ \frac{2g_e^4}{s^2} [A_1 Q_F^2] + \frac{g_Z^4}{8 [(M_Z^2 - s)^2 + M_Z^2 \Gamma_Z^2]} \right. \\ & \times \left[(C_A^{e^2} + C_V^{e^2}) (C_V^{F^2} A_1 + C_A^{F^2} A_2) + 4C_A^e C_A^F C_V^e C_V^F s A_3 \right] \\ & + \frac{g_{Z'}^4}{8 [(M_{Z'}^2 - s)^2 + M_{Z'}^2 \Gamma_{Z'}^2]} \left[(C_A'^{e^2} + C_V'^{e^2}) (C_V'^{F^2} A_1 + C_A'^{F^2} A_2) \right. \\ & \left. \left. + 4C_A'^e C_A'^F C_V'^e C_V'^F s A_3 \right] \right\} \end{aligned}$$

$$\begin{aligned}
& - \frac{g_e^2 g_Z^2 (-Q_F) (M_Z^2 - s)}{2s \left[(M_Z^2 - s)^2 + M_Z^2 \Gamma_Z^2 \right]} (C_A^e C_A^F s A_3 + C_V^e C_V^F A_1) \\
& - \frac{g_e^2 g_{Z'}^2 (-Q_F) (M_{Z'}^2 - s)}{2s \left[(M_{Z'}^2 - s)^2 + M_{Z'}^2 \Gamma_{Z'}^2 \right]} (C_A'^e C_A'^F s A_3 + C_V'^e C_V'^F A_1) \\
& + \frac{g_Z^2 g_{Z'}^2 [M_Z^2 (M_{Z'}^2 - s) + M_Z M_{Z'} \Gamma_Z \Gamma_{Z'} + s (s - M_{Z'}^2)]}{\left[(M_Z^2 - s)^2 + M_Z^2 \Gamma_Z^2 \right] \left[(M_{Z'}^2 - s)^2 + M_{Z'}^2 \Gamma_{Z'}^2 \right]} \\
& \times \left\{ C_A^e \left[C_A'^e (C_A^F C_A'^F A_2 + C_V^F C_V'^F A_1) + C_V'^e s A_3 (C_A^F C_V'^F + C_A'^F C_V^F) \right] \right. \\
& \left. + C_V^e \left[C_A^F (C_A'^e C_V'^F s A_3 + C_A'^F C_V'^e A_2) + C_V^F (C_A'^e C_A'^F s A_3 + C_V'^e C_V'^F A_1) \right] \right\}
\end{aligned}$$

where $A_1 = (s + t)^2 + t^2 - 4M_F^2 t + 2M_F^4$, $A_2 = A_1 - 4M_F^2 s$ and $A_3 = s + 2t - 2M_F^2$. The g_Z and $g_{Z'}$ are the coupling constants of the neutral current interactions with the gauge bosons Z and Z' , respectively. The $C_V'^F$ (C_V^F) and $C_A'^F$ (C_A^F) are vector and axial-vector couplings with the Z' (Z) boson. The s and t are Mandelstam variables. M_Z and $M_{Z'}$ are the masses of Z and Z' bosons; M_F is the heavy fermion mass. Γ_Z and $\Gamma_{Z'}$ are decay widths for Z and Z' bosons, respectively. In order to obtain the differential cross section depending on the scattering angle, $d\sigma/d\cos\theta$, the expression $d\sigma/dt$ should be multiplied by the factor $s\beta/2$ where $\beta = \sqrt{1 - 4M_F^2/s}$, and here we use $t = M_F^2 - s(1 - \beta\cos\theta)/2$.

Acknowledgments

The work is supported in part by Turkish Atomic Energy Authority (TAEK) under Grant No. CERN-A5.H2.P1.01-10. The work of O.C. and V.C. is supported in part by the State Planning Organization (DPT) under Grant No. DPT2006K-120470.

-
- [1] A. Lister, [CDF Collaboration], arXiv: 0810.3349 [hep-ex].
 - [2] T. Aaltonen *et al.*, [CDF Collaboration], Phys. Rev. Lett. **104**, 091801 (2010).
 - [3] C.J. Flacco *et al.*, arXiv: 1005.1077 [hep-ph].
 - [4] G.D. Kribs *et al.*, Phys. Rev. D **76**, 075
 - [5] J. Erler and P. Langacker, Phys. Rev. Lett. **105**, 031801 (2010).
 - [6] J.L. Hewett and T.G. Rizzo, Phys. Rept. **183**, 193 (1989).
 - [7] A. Leike, Phys. Rept. **317**, 143 (1999).

- [8] T.G. Rizzo, arXiv: hep-ph/0610104.
- [9] P. Langacker, arXiv: 0801.1345 [hep-ph].
- [10] K. Nakamura et al. (Particle Data Group), Jour. of Phys. G **37**, 075021 (2010).
- [11] J. Erler *et al.*, JHEP **0908**, 017 (2009).
- [12] V.M. Abazov *et al.* (D0 Collaboration), Phys. Rev. Lett. **100**, 142002 (2008).
- [13] T. Aaltonen *et al.* (CDF Collaboration), arXiv:1101.0034; T. Aaltonen *et al.* (CDF Collaboration), Phys. Rev. Lett. **101**, 202001 (2008).
- [14] The LEP Collaboration, Phys. Rept. **427**, 257 (2006).
- [15] A. Djouadi, G. Moreau and F. Richard, Nucl. Phys. B **773**, 43 (2007).
- [16] A. Djouadi *et al.*, arXiv: 0906.0604 [hep-ph].
- [17] E.L. Berger *et al.*, Phys. Rev. Lett. **106**, 201801 (2011).
- [18] C. Ciobanu *et al.*, *Z' generation with PYTHIA*, CDF/PHYS/EXOTICS/PUBLIC/7755 (2005).
- [19] J. Brau *et al.*, ILC Reference Design Report Volume 3, arXiv:0712.1950 [physics.acc-ph].
- [20] J. Brau *et al.*, ILC Reference Design Report Volume 2, arXiv:0709.1893 [hep-ph].
- [21] R.W. Assmann *et al.*, (The CLIC Study Team), CERN 2000-008; CERN-2003-007; for an update see http://clic-meeting.web.cern.ch/clic-meeting/CLIC_Phy_Study_Website/default.html.
- [22] E. Accomando *et al.*, (The CLIC Physics Working Group), CERN-2004-005, e-Print: hep-ph/0412251.
- [23] A. Pukhov *et al.*, Preprint INP MSU 98-41/542, arXiv:hep-ph/9908288; A. Pukhov, e-Print Archive: hep-ph/0412191.
- [24] G. Eilam, B. Melic and J. Trampetic, Phys. Rev. D **80**, 116003 (2009).
- [25] M. A. Schmidt and A. Y. Smirnov, arXiv:1110.0874 [hep-ph], (2011).